Received: 5 May 2017 | Revised: 22 October 2017 | Accepted: 27 October 2017

DOI: 10.1002/eqe.3005

RESEARCH ARTICLE

WILEY

Quantification of modelling uncertainty in existing Italian RC frames

Gerard J. O'Reilly[1] | Timothy J. Sullivan[2]

[1] Scuola Universitaria Superiore IUSS Pavia, Pavia, Italy

[2] Department of Civil and Natural Resources Engineering, University of Canterbury, Christchurch, New Zealand

Correspondence
Gerard J. O'Reilly, Scuola Universitaria Superiore IUSS Pavia, Pavia, Italy.
Email: gerard.oreilly@iusspavia.it

Summary

Assessment of the seismic performance of existing structures requires due consideration of both aleatory and epistemic sources of uncertainty; the former being typically associated with the randomness in ground motion records and the latter with the uncertainty in numerical modelling. Using a numerical modelling approach calibrated to available experimental test data collected from the literature, the uncertainty associated with different modelling parameters for existing reinforced concrete frames in Italy was quantified via an extensive numerical study. This was done to quantify the propagation of modelling parameter type uncertainty to the overall dispersion of the demand parameters typically used in seismic assessment, namely peak storey drift and peak floor accelerations. In addition, the impact of such modelling uncertainty on the median intensity and dispersion of the collapse fragility function was also examined. From the results of this study, empirical values of modelling parameter uncertainty were quantified with a view to being used in the assessment of existing reinforced concrete frames with masonry infill designed prior to the introduction of seismic design provisions in Italy during the 1970s. Comparing these empirical values to those available in the literature, it is seen how the fundamental behaviour of the frames differs from more modern frames with ductile detailing to the extent that values available in guidelines such as FEMA P58 cannot be reasonably adopted for these structural typologies.

KEYWORDS

assessment, collapse, dispersion, fragility, modelling uncertainty, RC frames

1 | INTRODUCTION

When assessing existing structures using either simplified methods or more advanced non-linear response history analyses (NRHA), the dispersion in the demand parameters of interest ought to be considered. Following the PEER performance-based earthquake engineering methodology,[1] where a single deterministic model is analysed using NRHA, epistemic uncertainty related to modelling uncertainty is incorporated into the analysis results together with the aleatory randomness due to record-to-record variability of the ground motion set used during the analysis, usually through a square root sum-of-the-squares (SRSS) combination. The inclusion of modelling uncertainty is of paramount importance in seismic assessment, with Gokkaya et al,[2] for example, remarking that incorporating modelling uncertainty in collapse assessment amplified the annual probability of collapse by approximately 1.8. Other analysis approaches, like displacement-based assessment[3] or pushover-based methods,[4,5] involve using simplifying methods to estimate the structural

response and a subsequent approximation of dispersion in the response. These aforementioned methods require some prescribed values of dispersion for modelling uncertainty that typically come from suitable quantification studies. Fajfar and Dolšek,[4] for example, emphasised that "For practical applications, predetermined default values for the dispersion measures, based on statistical studies of typical structural systems, are needed" and "...in a practice-oriented approach, default values for the dispersion measures have to be used. Reliable data for large populations of buildings are not yet available". While Fajfar and Dolšek[4] were referring to the dispersion measures that fit directly into the SAC/FEMA approach,[6] the issue remains the same that values for dispersion are needed for different structural typologies, whether they be for the estimation of the annual probability of exceedance of a given limit state similar to Fajfar and Dolšek,[4] or the annualised losses using the PEER performance-based earthquake engineering methodology implementation in FEMA P58.[7] In recent years, some studies[8-13] have quantified modelling parameter uncertainty for existing reinforced concrete (RC) frames, but these studies have tended to focus on either modern RC frames with ductile detailing or on older RC frames without masonry infill. Lastly, some more recent studies[14] on the loss estimation of gravity load designed (GLD) RC frames with masonry infill in Italy have tended to omit the inclusion of modelling uncertainty, highlighting the need for further investigation. To the authors' knowledge, no study that specifically addresses the dispersion due to modelling uncertainty on older RC frames with masonry infill typically found throughout Italy and the Mediterranean area exists in the literature.

This article aims to estimate and provide empirical values of dispersion due to modelling uncertainty that can be used when assessing GLD RC frames with masonry infill in Italy. Previous research on the topic is first examined, and some of the principal observations are summarised to provide insight into the different aspects to consider here. The methodology adopted to quantify modelling uncertainty is then outlined and applied to various GLD RC frame typologies so as to quantify empirical values of dispersion for both the collapse fragility and demand parameters, where the intensity measure employed for the collapse fragility was the spectral acceleration at the first-mode period of vibration of the structure, $Sa(T_1)$. This was done using the statistical information for the uncertainty in the different modelling parameters established during the recently proposed numerical model calibration for GLD RC frames with masonry infill by the authors.[15-18] These included the modelling of the beam and column members, beam-column joints, and masonry infill; all of which have been shown to be particularly vulnerable to damage during past earthquakes. These empirical values for dispersion due to modelling parameter uncertainty were segregated according to structural typology, demand parameter, and limit state under consideration to provide a set of empirical values for existing RC building typologies found throughout Italy.

2 | PAST RESEARCH QUANTIFYING MODELLING UNCERTAINTY

2.1 | Overall effects of modelling uncertainty

One of the goals of examining the modelling uncertainty is to study its overall influence with respect to the randomness associated with record-to-record variability. Research to date naturally agrees that the inclusion of modelling uncertainty increases the overall uncertainty of the system (eg, Dolšek[8] and Liel et al[19]), but to what extent with respect to record-to-record variability has not been consistent. Early studies by Ellingwood et al[20] elected to neglect the effects of modelling uncertainty as previous research by Kwon and Elnashai[21] suggested that compared with the record-to-record variability, the dispersion associated with uncertainty in material properties does not appear to be significant. Dolšek[22] discussed the influence of modelling uncertainty with respect to risk because the discussion thus far in the literature had referred to different limit states and not considered the combination with a given hazard curve to discuss the actual implications on risk. Dolšek[22] concluded that the effects of modelling uncertainties, in addition to record-to-record variability, increase with the severity of the limit state such that, for the near collapse limit state, the risk considering both sources of uncertainty is more than double if compared with the risk determined solely from record-to-record variability. More recently, Kosič et al[12,13] have examined the relative values of dispersion due to record-to-record variability and modelling uncertainty in RC frames newly designed using Eurocode 8[23] and older RC frames without seismic design provisions; both of which were without consideration of the presence of masonry infill. Their work closely resembles some of the work outlined in this article, and their work showed the general magnitude of the dispersion to be of comparable magnitude for the 2 aforementioned sources of uncertainty in seismic assessment.

Bradley[24] discussed the current state-of-the-art in terms of quantifying modelling uncertainties and noted that studies to date have typically focused on variability in constitutive model parameters, with no consideration of more modelling approaches on a higher, more conceptual level. This is typically referred to as model type uncertainty,[25] whereas the

focus in this paper is on model parameter uncertainty. The point made by Bradley[23] appears valid when one considers, for example, the dispersion in results from different analysts observed in blind-prediction test results of a single bridge pier by Terzic et al.[26] In order to examine these considerations in numerical modelling, a large coordinated parametric study would be required to adequately reflect this source of uncertainty, but this is not within the scope of this work, which instead focuses on the quantification of the modelling parameter type uncertainty.

2.2 | Previous investigation into the effects of random variables

Of the numerous studies regarding modelling uncertainty available in the literature, one of the more critical aspects is the initial identification of appropriate and relevant random variables (RVs) to employ. The methods used and subsequent assumptions can require very computationally expensive procedures involving simulation to generate a sufficient number of realisations followed by NRHA that somewhat limit the possibility of comprehensive studies on the topic. Hence, past research on the topic is first discussed here to provide an insight into the relative impact on the structural response of different RVs.

Some studies[8-11] have examined how uncertainty in characteristic material properties in RC frames and the mass distribution affects the dispersion in fragility functions and, in general, have reported that these have limited effect on the dispersion when compared with other RVs. For example, Dolšek[8] demonstrated that the elastic damping and the ultimate rotation capacity of the frame members are the most influential RVs. Such findings are further reflected in the comments by Liel et al[19] who, when referring to work by Haselton and Deierlein,[27] noted that concrete and steel material strengths have been shown in the past to have limited influence on the collapse limit state compared with the deformation capacity and post-peak stiffness of the frames members, which were shown to have a major role, as also observed in the extensive parametric studies conducted by Ibarra et al.[28] Liel et al[19] then demonstrated through a sensitivity study that column strength and ductility are the most influential RVs for RC frames without masonry infill. These findings regarding the influence of strength and ductility of frame members were also echoed in the work of Vamvatsikos and Fragiadakis.[29]

With regard to elastic damping, some studies[19,27] have indicated that its effect is relatively minimal, while others[8,9] have noted its importance. In terms of the relative influence of the parameters at the collapse limit state, this minimal impact may be the case where the uncertainty in the peak and post-peak deformation capacity dominate the response. Because the present study considered the entire range of structural response including collapse, and considering the results of past sensitivity studies (eg, O'Reilly and Sullivan[17]), the elastic damping was considered an uncertain parameter that merited consideration. In addition to the RC frame elements, some other modelling parameters pertaining to this study were the relative importance of the beam-column joint and masonry infill properties. Celik and Ellingwood[9] conducted a sensitivity study on a number of parameters for non-ductile RC frames where, in addition to the elastic damping, the shear strain at cracking in the beam-column joints was shown to be a key parameter. Similarly, Celarec et al[11] performed a sensitivity study on older RC frames with masonry infills and showed that for lower limit states, the uncertainty in the masonry infill properties had the largest impact, whereas at limit states closer to the collapse of the structure, the ultimate chord rotation capacity of the beam and column members played a more significant role.

Kosič et al[12,13] noted that for older RC frame buildings, an additional human-induced uncertainty arises due to the imperfect knowledge of the actual structural composition because very little structural detail may be available. Jalayer et al[30] suggested that the quantity of reinforcement should also be considered an RV as this could arise due to human error from placing an incorrect bar diameter size during construction. Furthermore, when performing an assessment of an older RC frame, the section details are often not available and an engineer is faced with either conducting a simulated design to estimate what the structural engineer at the time would have provided, assume a reasonable percentage of reinforcement based on engineering judgement or conduct in-situ testing to determine the actual reinforcement present. The latter approach is much more costly and invasive and may not be possible for various reasons, while the former 2 approaches introduce a significant uncertainty to models when one considers how the reinforcement content impacts the member strength, which has been previously shown to be a key parameter.

2.3 | Effects of modelling uncertainty on median demands and collapse performance

While the effects of modelling uncertainty on the overall dispersion have been recognised, the effects on the median demands and collapse performance provide some extra food for thought. This is because one of the underlying assumptions in assessment guidelines to assess demands, such as the SAC/FEMA guidelines,[6] and the FEMA P695 guidelines[31]

to assess collapse performance are that modelling uncertainty increases the overall dispersion but the median demands remain unchanged. In the case of the structural demands, Dolšek[8] noted how the median drift demand of an RC frame remained unchanged far from collapse when modelling uncertainty effects were considered. In the case of the collapse performance, however, numerous studies[2,8,13,19,29] have indicated that the inclusion of modelling uncertainty tends to reduce the median collapse intensity from that observed when using a deterministic model with median value parameters. Vamvatsikos and Fragiadakis[29] have noted this to be as a result of the "weakest link" concept, where the possibility of sampling an unusually weak component in the structural system results in an overall reduction of the median collapse intensity with respect to a deterministic model. This reduction in median collapse capacity was also seen from the work of Kosič et al[13] who noted a difference in the pushover curve of the deterministic model and the mean pushover curve of the sampled building models. They reported a reduction in ductility capacity in the older RC frames, which when considering the relationship between a structure's pushover and incremental dynamic analysis (IDA) curve from Vamvatsikos and Cornell,[32] would translate as a reduction in median collapse capacity. Both Liel et al[19] and Gokkaya et al,[2] for example, noted this reduction in the median collapse intensity to be up to 20%, with the reduction being more pronounced for non-ductile frames compared with modern ductile frames.

3 | STRUCTURAL TYPOLOGIES AND NUMERICAL MODELLING

The case study frames discussed herein consisted of 2 and 3 storey RC frames that were adopted from a previous study by Galli.[33] Both frames were designed for gravity loads only using allowable stress and other such design provisions outlined in Regio Decreto 2229/39,[34] along with other common construction conventions prior to the introduction of seismic design provisions in Italy in the 1970s, which are summarised in Vona and Masi.[35] Some typical characteristics of these GLD RC frames are the complete lack of capacity design considerations in the beam and column members, as the columns were sized principally for axial loading and the beam members were typically designed by considering the hogging and sagging moments of a continuously loaded beam on multiple supports. This approach was quite common during the construction boom that followed the second world war across southern Europe and resulted in many RC structures being vulnerable to undesirable seismic response. In addition to the out-of-date seismic provisions (or in many cases, no seismic provisions at all) adopted during past construction, another detail regarding the construction of these buildings that leaves them quite vulnerable to seismic loading was the use of smooth reinforcing bars in the frame members that were terminated with end-hooks in the beam-column joints. This affects the bonding of the reinforcement to the concrete and results in a modified ductility compared with newer ductile detailing of the frame members, in addition to the increased risk of a potential shear mechanism in beam-column joints, as discussed in O'Reilly and Sullivan.[15]

Figure 1 illustrates a typical GLD RC frame with masonry infill along with some of its most vulnerable components. The case study frames examined herein consisted of a 3-bay frame with exterior bays of 4.5 m and an internal bay of 2 m, a constant storey height of 3 m, and out-of-plane tributary width of 4.5 m. The strength of the reinforcing steel and concrete were 3800 kg/cm^2 (372 MPa) and 200 kg/cm^2 (19.6 MPa), respectively, whereas the floor loadings were taken as 500 kg/m^2 for the roof levels and 600 kg/m^2 for each floor, as per typical design manuals in use at the time of construction.[33] As these frames were sized for gravity loading only, the beam section sizes and detailing were constant at each level in addition to the column sections. The column sections consisted of 25 × 25 cm sections with four 14-mm longitudinal bars and 6-mm transverse stirrups placed every 100 mm. The beam sections consisted of a 25 × 50 cm deep rectangular section with four and two 14 mm longitudinal bars placed at the top and bottom, respectively, also with 6-mm transverse stirrups placed every 100 mm.

In terms of numerical modelling of the case study frames, the developments of the authors[15-17] using the OpenSees framework[38] were adopted herein for the structures. The beam and column elements were modelled using a lumped plasticity element, and the hysteretic rule for these is illustrated in Figure 1. The different parameters required for the beam-column element model were determined from the calibration with existing experimental test data outlined in O'Reilly and Sullivan[15] to adequately capture the behaviour of the older RC frames discussed here. The beam-column joints were modelled using a zero-length hinge at the joint centres to characterise the vulnerability of these to brittle shear failure as a result of no transverse shear reinforcement in the joint region. The hysteretic rule for the beam-column joint model is illustrated in Figure 1, and similar to the beam-column elements, the various terms were taken from the calibration study outlined in O'Reilly and Sullivan[15] for these types of joints typically found in older RC frames. To incorporate the effects of masonry infill, the equivalent diagonal strut model outlined in Crisafulli et al[39] was adopted, and the

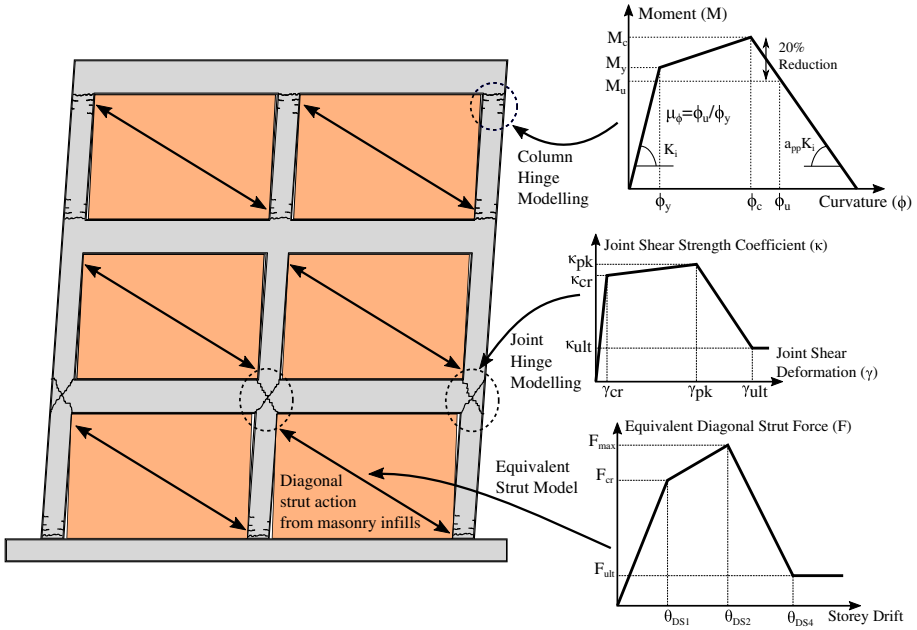

FIGURE 1 Illustration of the numerical modelling of the various damageable components of GLD RC frames with masonry infills. The hysteretic behaviour of the beams, columns, beam-column joints, and masonry infill struts are also illustrated (see Table 2 for list of symbols) [Colour figure can be viewed at wileyonlinelibrary.com]

hysteretic backbone parameters proposed by Sassun et al[36] for the hysteretic backbone of these struts shown in Figure 1 were utilised. The floor system was modelled using a rigid diaphragm, which was deemed a reasonable assumption for the "laterizio" floor systems[40] that were quite common in Italy during that period.

While the case study frames were designed as bare frames, common practice throughout Italy was to insert masonry infills in the structures without considering their effects on the surrounding frame during the design process. As such, a number of different infilled case study frames were also investigated to illustrate their effects on the structural behaviour and overall performance of GLD RC frames. Two different infill layouts were considered; a uniform infill throughout the height of the building and a uniform infill layout with an open ground storey—commonly referred to as a "pilotis" frame. These pilotis frames were, and still are, quite popular throughout Italy as they offer large open areas suitable for retail space at the ground storey, while the upper storeys tend to be for residential use. In addition to the uniform infill and pilotis frames, 2 types of masonry infill were used herein and were termed "weak" and "strong" infill, as per Hak et al,[41] where weak infill denoted 8-cm-thick single leaf infill and strong infill implied 30-cm-thick block. These were adopted in order to illustrate the effects of different infill typology on the seismic behaviour and overall performance of the structure. The effects of modelling openings such as windows or doors were not considered as part of this study. Table 1 lists each of the model variations along with the first-mode period of vibration of each deterministic model.

These different structural typologies, consisting of frames modelled without infill, frames with a pilotis configuration, and frames with full infills considering 2 masonry typologies, were examined so as to permit values of dispersion associated with modelling parameter uncertainty for the various structural frame typologies typically found in Italy to be quantified.

TABLE 1 List of each structural typology examined and the first-mode period of the deterministic model

Structural Typology	2 Storey	3 Storey
W/o infill	0.82 s	1.19 s
Pilotis frame	0.62 s	0.75 s
Infill frame (strong)	0.15 s	0.21 s
Infill frame (weak)	0.24 s	0.36 s

4 | METHODOLOGY

As discussed previously in Section 2, the variability in the different modelling parameters is propagated through the structural response to result in a variability in the demand parameters of interest. This is in conjunction with the inherent variability due to record-to-record variability when performing NRHA. While the record-to-record variability is typically accounted for with large sets of suitable ground motions, the modelling uncertainty is somewhat more difficult to quantify. This is because the individual distributions of the various RVs in the structure are required along with an appropriate method with which a number of different numerical model realisations can be generated. As outlined previously, a common approach is to empirically quantify the effects of this modelling uncertainty on the various demand parameters of interest and incorporate their effects during the post-processing of analysis results alongside the record-to-record variability. This section, therefore, aims to outline a methodology with which to quantify the dispersion due to modelling uncertainty for different demand parameters such as peak storey drift (PSD) and peak floor acceleration (PFA) in existing GLD RC frame structural typologies with masonry infill found throughout Italy.

4.1 | Overview

A schematic representation of the procedure followed herein is illustrated in Figure 2 where for each of the structural typologies described in Section 3, a number of model realisations were generated to take the variability of the different considered RVs into account. These model realisations were then analysed using IDA[42,43] at a number of intensity levels so that the dispersion can be examined as a function of intensity and demand parameter of interest. That is, the dispersion due to modelling uncertainty in the PSD and PFA with respect to intensity is quantified in addition to the dispersion in collapse capacity.

In addition to quantifying the dispersion due to modelling uncertainty as a function of intensity, Figure 2 also illustrates how the exceedance of global limit states in the buildings were identified using static pushover analysis. This meant that the dispersion values identified in later sections could be adopted with respect to the limit state rather than solely as a function of intensity. This is similar to what is done in FEMA P-58[7] where the prescribed dispersion values are provided as a function of the different ranges of global structural response. The distinction provided here in terms of limit state is intended to provide a similar refinement that would be familiar to practicing engineers using more simplified methods of analysis, such as simplified loss estimation using displacement-based assessment outlined in Sullivan et al,[44] or more refined analysis such as that outlined in O'Reilly and Sullivan,[45] for example. These limit states were defined in accordance with the definitions outlined in the Italian National Code NTC 2008,[46] which defines 4 limit states: Operational (SLO), Damage Control (SLD), Life Safety (SLV), and Collapse Prevention (SLC), respectively, which are illustrated qualitatively in Figure 3. These were identified as per Figure 3B using static pushover analyses carried out in O'Reilly and Sullivan[45] to identify the critical PSD associated with each limit state for the different structural typologies. As illustrated in Figure 2, these critical PSD values were then combined with the IDA curves of the deterministic model outlined in O'Reilly and Sullivan[45] to establish a median intensity at which the different limit states are exceeded. Knowing this median intensity for each limit state, the dispersion due to modelling uncertainty quantified here can be expressed relative to these limit states of the structure also.

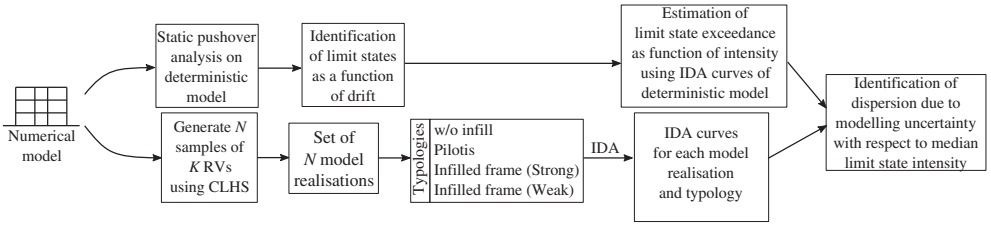

FIGURE 2 Schematic representation of the procedure used herein to identify the dispersion due to modelling uncertainty in various structural typologies with increasing intensity

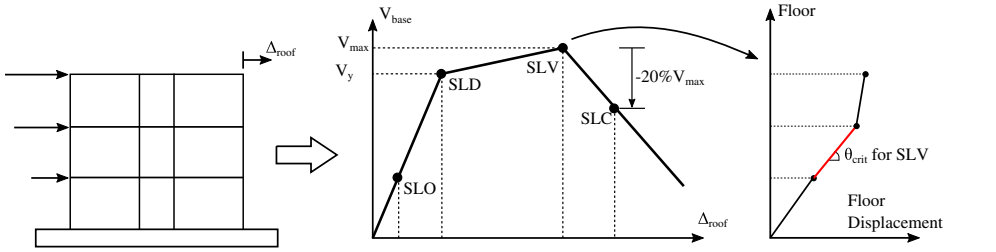

FIGURE 3 Illustration of static pushover analysis and subsequent identification of different limit states according to NTC 2008, for the structural typologies considered [Colour figure can be viewed at wileyonlinelibrary.com]

4.2 | Selected random variables and associated distributions

Based on the discussions of Section 2 and the numerical modelling of the different structural typologies described in Section 3, the RVs selected as part of this quantification study for GLD RC frames typically found in Italy were established, and a brief description of the source of such information and the relevant justification for their consideration is outlined. Table 2 lists the RVs selected for each of the beam and column frame members, interior and exterior beam-column joints, masonry infill, and other global modelling parameters. References to sources that support the adoption of each of the RV values are included, where the RVs outlined are also illustrated for the different components in Figure 1. In cases where no data were available to determine a suitable value of dispersion for the joints and masonry infill, expert judgement was used.

The beam and column member distributions were adopted directly from the information presented in O'Reilly and Sullivan,[15] because the information regarding the member capacity, stiffness, and ductility capacity come from the calibration to actual test data available in the literature. The noted source of "computed" for the members in Table 2

TABLE 2 List of RVs considered for quantification of dispersion due to modelling parameter uncertainty in GLD RC frames, where the median value and corresponding dispersion value are provided for the lognormal distribution of each (notation is as per model definitions in O'Reilly and Sullivan[15] and illustrated in Figure 1)

RV			Description	Source	Median	Dispersion	Reference
1,6	Beams and Columns	M_y	Yield moment	Computed	-	0.122	[15]
2,7		φ_y	Yield curvature			0.287	
3,8		μ_φ	Ultimate curvature ductility			0.326	
4,9		a_{pp}	Post-peak stiffness ratio			0.413	
5,10		ρ_L	Longitudinal reinforcement ratio			0.250	
11	Exterior joints	γ_{cr}	Joint shear deformation at cracking	Test data	0.0002	0.300	Estimate [15]
12		γ_{pk}	Joint shear deformation at peak capacity		0.0127	0.286	
13		γ_{ult}	Joint shear deformation at ultimate capacity		0.0261	0.229	
14		κ_{cr}	Joint shear strength coefficient at cracking		0.135	0.166	
15		κ_{ult}	Joint shear strength coefficient at ultimate capacity		0.05	0.091	
16	Interior joints	γ_{cr}	Joint shear deformation at cracking	Test data	0.0002	0.300	Estimate [15]
17		γ_{pk}	Joint shear deformation at peak capacity		0.0085	0.133	
18		κ_{cr}	Joint shear strength coefficient at cracking		0.29	0.237	
19		κ_{pk}	Joint shear strength coefficient at peak capacity		0.42	0.163	
20	Masonry infills	F_{max}	Infill diagonal strut capacity	[36]	-	0.300	Estimate [36]
21		θ_{DS1}	Storey drift at DS1 defined in[36]	Test data	0.18%	0.520	
22		θ_{DS2}	Storey drift at DS2 defined in[36]		0.46%	0.540	
23		θ_{DS4}	Storey drift at DS4 defined in[36]		1.88%	0.380	
24	Global	ξ	Elastic damping ratio[a]	Assumed value	0.05	0.600	[37]
25		M	Floor mass	Given	-	0.100	

[a]Modelled as tangent stiffness-proportional Rayleigh damping.

refers to how the median value was not a fixed value but rather a computed value from the expressions described in O'Reilly and Sullivan[15] (eg, the yield moment (M_y) was not a fixed value for every member, but depended on section dimensions, axial load ratio, and reinforcing content) and the associated dispersion values were computed from the comparison of the relevant expression to the actual test data. Other information regarding masonry infill median drifts and dispersions were adapted from the study by Sassun et al,[36] whereas other information regarding appropriate dispersions for elastic damping and structural mass were adopted from a similar study conducted by Haselton et al.[37]

Also of note were the correlations assumed between different RVs. Past studies, such as Haselton et al,[37] describe 2 types: inter-component and intra-component correlation. The latter refers to correlation between RVs associated with a single structural element (eg, yield curvature and post-peak stiffness of a single column member) whereas the former refers to the correlation between the RVs of different elements (eg, yield moment of a beam and infill diagonal strut capacity). All of the structural elements were sampled together and not considered individually (eg, the sampled value of column yield curvature was assumed to be equal in each column member) meaning that each element type was fully inter-correlated. Considering these elements individually would have resulted in a very large number of RVs and drastically increased the number of model realisations required (see Section 4.3), meaning that the study would have been unfeasible from a numerical computation perspective, although it is noted here that incorporating the recent work by Vamvatsikos[47] that has also been applied in Kazantzi and Vamvatsikos[25] could overcome this in future studies. Additionally, the approach outlined in Kosič et al[13] via the use of equivalent single degree of freedom oscillators could overcome this numerical computation hurdle in future work.

The RVs associated with different structural elements (eg, interior beam-column joints and columns) were assumed here to be independent and uncorrelated. Physical relations between different RVs were maintained through the model definition (for example, considering the yield moment and the percentage of reinforcement, the yield moment was automatically computed using the sampled value of reinforcement through sectional analysis). Regarding the intra-element correlations between RVs of single elements, past studies[2,8,12,13,25,37] have assumed some kind of correlation between the various terms. Available experimental data can provide an indication of a suitable correlation coefficient whereas in other situations when insufficient experimental data is available, expert opinion and mechanics-based reasoning to determine suitable values is required. Haselton et al,[37] for example, noted that the 30 experimental test specimens available to them at the time were too few to identify suitable coefficients and relied on expert judgement instead. Ugurhan et al[48] later calibrated correlation coefficients from the experimental test database consisting of over 200 test specimens described in Haselton et al,[49] and these were subsequently used in the later study by Gokkaya et al.[2] The approach adopted here was a combination of using available experimental test data and expert opinion depending on the availability of suitable data. For the masonry infill, experimental test data for 50 specimens collected in Sassun et al[36] were used to determine the correlation coefficients between the limit state drift values used in the equivalent diagonal strut model. For the beam-column and joint elements, experimental test data collected and reported in O'Reilly and Sullivan[15] were used to compute correlation coefficients between the various terms. Due to the limited number of test specimens described in O'Reilly and Sullivan[15] for GLD RC frame elements, the computed correlation coefficients were reviewed to ensure that no spurious correlation due to the lack of sufficient test data arose. This represents an aspect of this study that may be improved in future studies when more experimental data become available to determine suitable coefficients more accurately. Using the above information, the correlation matrix for the RVs listed in Table 2 was identified and is plotted in Figure 4A, where the RV numbers are as listed in the first column of Table 2.

4.3 | Generation of model realisations

In order to examine the modelling uncertainty in the response of a structural system due to a set number of RVs whose distributions were known or can be estimated, a number of model realisations needed to be generated. That is, for each RV considered, a random sample from its distribution was obtained and input to the structural model to create what is termed a single model realisation. For completeness, a model with median values for each RV is referred to herein as the deterministic or reference model. To generate such random samples for each RV, a Latin Hypercube Sampling technique[50] was employed along with some modifications outlined in Olsson et al[51] to reduce spurious and unintentional correlations between the RVs. The process is summarised as follows. Consider K number of RVs for which N number of realisations are to be generated. A random permutations matrix $\boldsymbol{P}$ of size N by K is first generated, such that each column corresponds to a different RV and consists of a random permutation of the integers 1 through N (this operation can be performed in MATLAB[52] using the command randperm). The next step is to generate a random matrix $\boldsymbol{R}$ of size N by K, such that each entry is sampled from the uniform distribution and is between 0 and 1 (performed using the rand

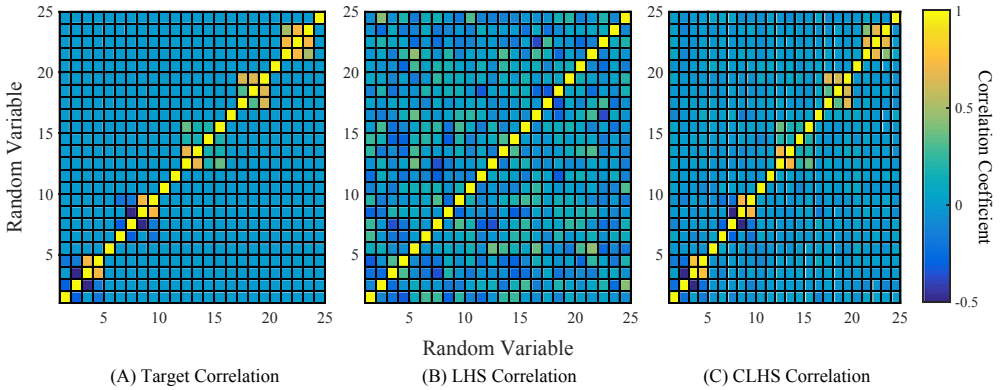

FIGURE 4 Plot of correlation coefficients between each of the RVs, where (A) illustrates the target correlation matrix, (B) shows the spurious correlation obtained when using a standing Latin hypercube sampling approach, and (C) shows a correlation matrix using the correlation-reduced Latin hypercube sampling approach to match the target correlation matrix outlined below [Colour figure can be viewed at wileyonlinelibrary.com]

function in MATLAB). Combining these 2 matrices $\boldsymbol{P}$ and $\boldsymbol{R}$, the basic Latin Hypercube Sample matrix $\boldsymbol{S}$ of the RVs, as indicated in Olsson et al,[51] is obtained by performing:

$$\boldsymbol{S}(n,k) = \frac{1}{N}\left(\boldsymbol{P}(n,k) - \boldsymbol{R}(n,k)\right) \tag{4.1}$$

whose elements are in the range of 0 to 1. Using these samples in $\boldsymbol{S}$ and the known distribution of each RV, a sample can be obtained using the RV's distribution to generate the RV sample matrix $\boldsymbol{X}$, as illustrated in Figure 5. As such, each entry in the matrix $\boldsymbol{X}$ corresponds to the sample value to be used in the structural system, where each column of $\boldsymbol{X}$ corresponds to a RV, and each row of $\boldsymbol{X}$ corresponds to a single realisation.

Using this approach, the required number of realisations may be sampled for any number of RVs. However, it can unintentionally introduce spurious correlations between different RVs as a result of them having been sampled independently, which is reflected in the correlation matrix for $\boldsymbol{S}$, $\boldsymbol{\rho_S}$. For example, if one were to examine the correlation between 2 RVs such as steel yield strength and masonry infill strength, one could find a strong positive correlation between these RVs in the generated sample matrix $\boldsymbol{S}$. Such a correlation obviously has no real basis and is not intentional but arises due to the way the samples were generated. As described in Olsson et al,[51] the random permutations matrix $\boldsymbol{P}$ is modified to address these spurious correlations that arise in Latin Hypercube Sampling using what is termed by Olsson et al[51] as Correlation-Reduced Latin Hypercube Sampling, and is summarised below.

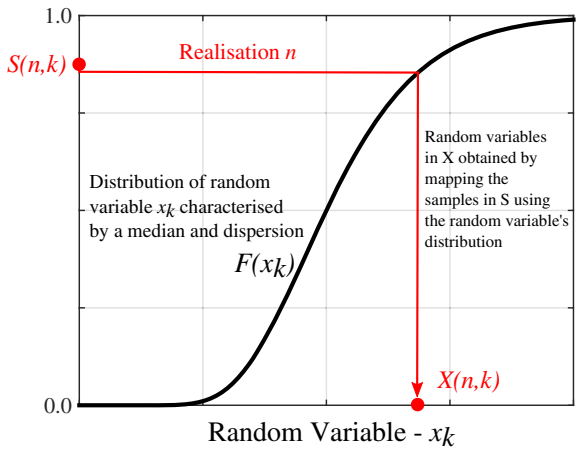

FIGURE 5 Generation of random samples X from the basic Latin hypercube sample S [Colour figure can be viewed at wileyonlinelibrary.com]

The approach outlined in Olsson et al[51] follows the work of Owen[53] where a matrix $\boldsymbol{Y}$ of size N by K is first identified by taking the random permutations matrix $\boldsymbol{P}$ and mapping it onto a Gaussian distribution with mean 0 and standard deviation of 1. The covariance matrix of $\boldsymbol{Y}$ is then computed and its Cholesky decomposition found to give:

$$\boldsymbol{L}\boldsymbol{L}^T = \mathrm{cov}(\boldsymbol{Y}) \tag{4.2}$$

where $\boldsymbol{L}$ is the lower triangle Cholesky decomposition (using the command chol in MATLAB). The process requires that the covariance matrix of $\boldsymbol{Y}$ be positive definitive, which essentially means that the number of required realisations should exceed the number of RVs (ie, $N > K$), although a more recent proposal by Vamvatsikos[47] introduces an alternative sampling approach that removes such a constraint. The next step is to compute a new matrix $\boldsymbol{Y}^*$ with a sample covariance given by:

$$Y^* = Y\left(L^{-1}\right)^T \tag{4.3}$$

and from $\boldsymbol{Y}^*$ a sample matrix $\boldsymbol{S}^*$ is generated by following the previous operation mapping $\boldsymbol{Y}$ to $\boldsymbol{P}$ and subsequently finding $\boldsymbol{S}$ as per Equation 4.1 in reverse.

However, if a target correlation ($\boldsymbol{\rho}$) between the RVs is required, then the above operation is modified such that:

$$Y^* = Y\left(L^{-1}\right)^T W^T \tag{4.4}$$

where $\boldsymbol{W}$ is the lower triangle Cholesky decomposition of the target correlation matrix $\boldsymbol{\rho}$.[53] As mentioned, this $\boldsymbol{Y}^*$ matrix is then converted back to a new random permutations matrix $\boldsymbol{P}^*$, which is in turn used to generate a new sample matrix $\boldsymbol{S}^*$, which is used in conjunction with the RV's known distributions to generate the samples $\boldsymbol{X}^*$ for the structural system. If one computes the original correlation matrix $\boldsymbol{\rho_S}$, the spurious correlations between the different RVs will be obvious from the off-diagonal terms of $\boldsymbol{\rho_S}$. Recomputing the correlation matrix for the correlation reduced sample $\boldsymbol{S}^*$, $\boldsymbol{\rho_{S^*}}$, it can be seen how such spurious correlations have been reduced.

Using this CLHS approach, a number of realisations of each structural model discussed in Section 3 were developed. Each of the 25 RVs listed in Table 2 was sampled a number of times to generate N number of model realisations whilst also considering the correlation between these samples, which are illustrated in Figure 4. The benefit of using the CLHS outlined here to generate the samples can be clearly seen from the matching of Figure 4A,C, where the spurious correlations observed in Figure 4B from using just LHS are effectively reduced through the CLHS approach. While each of the RVs is sampled according to the aforementioned distributions, care was taken to ensure that no instances of unrealistic model realisations arise. For instance, the sampled value of masonry infill damage state two, θ_{DS2}, was checked to be always greater than that of the drift of damage state one, θ_{DS1}. Other checks on the beam-column joint rotation samples were also applied in addition to the joint shear strength coefficients. As mentioned previously, the number of model realisations needed to be greater than the number of RVs (ie, $N > K$) in order for the sampling method to function. As such, 40 realisations were adopted here. This number was selected based on the findings of a parametric study by Dolšek,[8] who noted that 20 model realisations appeared to be reasonable, whilst also recognising that a number greater than 25 is required here. Therefore, 40 was judged to be a reasonable value.

For each of the model realisations sampled, the structural typologies discussed previously were analysed using 10 ground motions taken from the FEMA P695[31] far field set. These 10 ground motions were selected in order to maintain a good match in terms of mean and dispersion with the original set of 44, while maintaining computational efficiency for the adopted approach. Each ground motion was scaled to a number of intensities for the intensity measure (IM) employed for IDA, which was the spectral acceleration at the first-mode period of vibration of the structure, $Sa(T_1)$.

5 | ANALYSIS RESULTS

5.1 | Collapse fragility

By analysing the different structural typologies at different intensity levels via a truncated IDA, the number of collapses with respect to intensity, ground motion, and model realisation were identified. Using the maximum likelihood fitting method described by Baker,[54] the collapse fragility function of the different structural typologies was computed with respect to each ground motion record or model realisation as a function of intensity. Collapse is typically defined qualitatively as when the IDA trace "flatlines" or becomes sufficiently large to cause dynamic instability. This point was

defined quantitatively as when the maximum PSD exceeded 10% during analysis, which was deemed sufficiently large to have caused collapse and is consistent with other studies such as Gokkaya et al,[2] for example. These collapse fragilities are plotted in Figure 6 for each of the structures considered, where the plot labels correspond to:

- RTR—collapse fragilities considering record-to-record variability only.
- MDL—collapse fragilities considering modelling uncertainty only.
- TOT—collapse fragilities considering both record-to-record variability and modelling uncertainty.

As discussed previously in Section 4.1, the RTR line plotted in Figure 6 corresponds to the collapse fragility function obtained using the deterministic model of each case study structure.

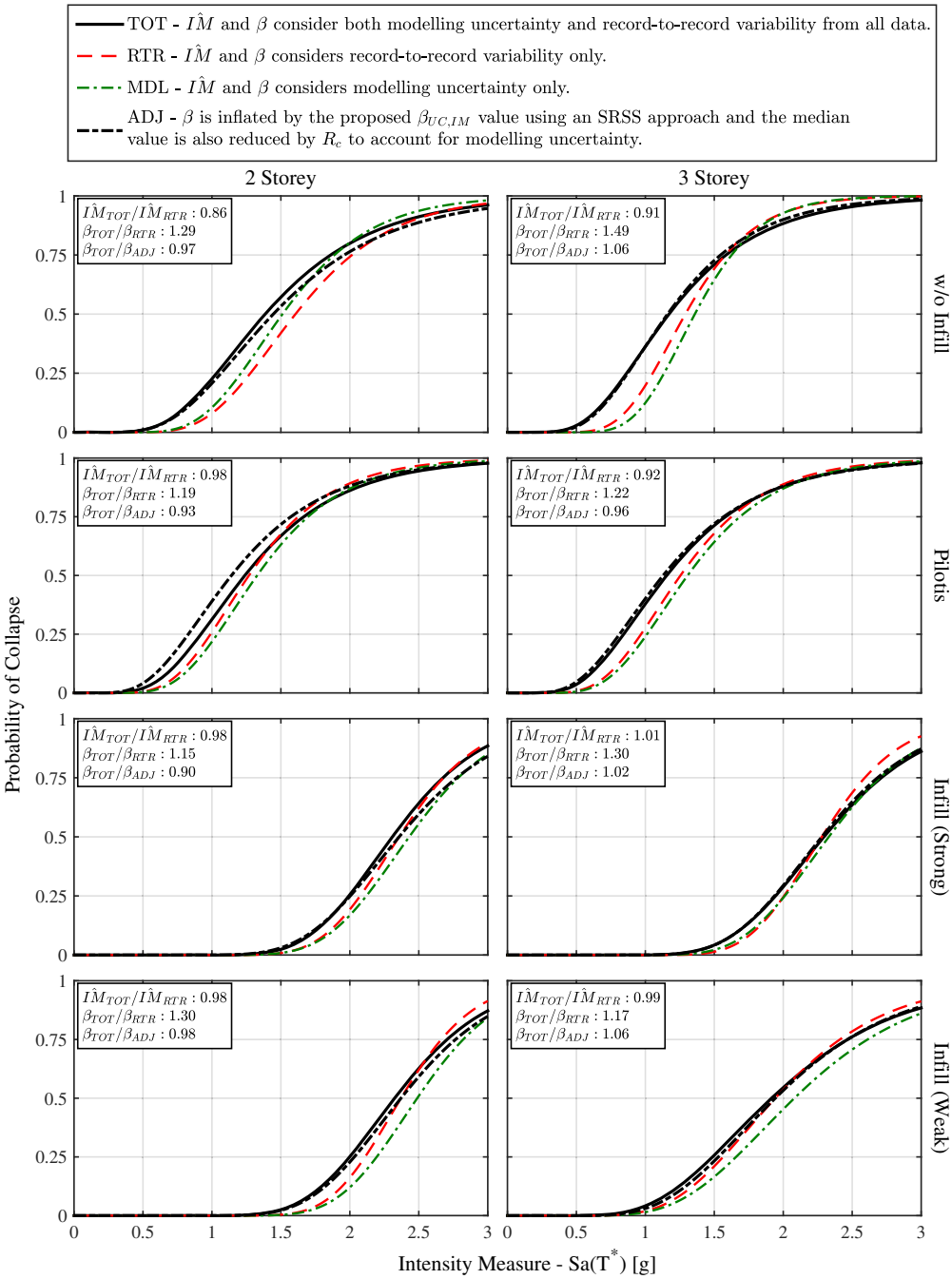

FIGURE 6 Comparison of the collapse fragility functions considering different sources of uncertainty compared with the 2 methods of adjusting the collapse fragility function to account for modelling uncertainty in GLD RC frames. Left and right-hand plots correspond to the 2 and 3 storey frames, respectively [Colour figure can be viewed at wileyonlinelibrary.com]

Taking the TOT as the most representative collapse fragility function, the ratios of median collapse intensity plotted in Figure 6 and listed in Table 3 can be seen to differ somewhat. The mean ratio of TOT to RTR for the median collapse intensity is 0.95 meaning that for all typologies examined, the RTR fragility functions tended to overestimate the median collapse intensity when compared with the collapse fragilities that account for both aforementioned sources of uncertainty, a finding consistent with existing research reviewed in Section 2. However, guidelines such as FEMA P695[31] do not propose a modification to the median value when accounting for modelling uncertainty, despite Figure 6 (and previous work) illustrating that this may not be conservative. In light of this, the approach proposed here is to provide adjustment factors for the median collapse intensity (R_c) as a function of structural typology using the data listed in Table 3. These proposed adjustments are listed in Table 3 and were computed using the mean ratio of the TOT to RTR cases for each structural typology. Compared with existing values in the literature, such as those proposed by Gokkaya et al,[2] for example, bare non-ductile frames with no masonry infill in the US were shown to be somewhat similar to the corresponding values in Table 3, where an average reduction of 0.95 was noted. It was noted that the values of R_c for infilled frames reported in Table 3 are relatively high compared with other typologies. This may be because the infill frame response tends to be dominated by the presence of the infill, and less so by the actual surrounding RC frame. Therefore, there were fewer RVs influencing the response of the frames as the variability mainly stems from the infill and not the frame elements such as beams, columns, and joints that possess many more RVs. This hypothesis, however, would require confirmation through more detailed sensitivity studies.

In addition to the median collapse intensity, Figure 6 illustrates how compared with the TOT fragility curves, the RTR curves tended to underestimate the total dispersion. The mean ratio of the TOT to RTR dispersion was found to be 1.27. This difference was an expected result and is typically accounted for by inflating the collapse dispersion by a prescribed value to account for the effects of modelling uncertainty. This is the approach of the FEMA P695 guidelines, among others, that prescribe values with which the RTR collapse fragility is to be increased using an SRSS combination. The dispersions plotted in Figure 6 for RTR and MDL are also listed below in Table 4. First examining the magnitude of the dispersion due to modelling uncertainty relative to those due to record-to-record variability, they are seen to be of similar magnitude, a finding also noted by others in Section 2. As previously outlined, the typical approach is to combine these 2 sources of uncertainty using an SRSS combination. The SRSS combination is also listed in Table 4, and when compared with the TOT values, it tends to overestimate the total dispersion.

TABLE 3 Median collapse intensities for different structural typologies accounting for total dispersion due to record-to-record variability and modelling uncertainty, and record-to-record variability alone, along with the proposed collapse fragility modification factors to account for the effects of modelling uncertainty on the median collapse intensity

Structural Typology	TOT		RTR		TOT/RTR		Proposed Median Reduction Factor (R_c)
	2 Storey	3 Storey	2 Storey	3 Storey	2 Storey	3 Storey	
W/o infill	1.39 g	1.17 g	1.61 g	1.29 g	0.86	0.91	0.89
Pilotis	1.24 g	1.15 g	1.27 g	1.25 g	0.98	0.92	0.95
Infill frame (strong)	2.31 g	2.30 g	2.36 g	2.28 g	0.98	1.01	0.99
Infill frame (weak)	2.33 g	1.92 g	2.37 g	1.94 g	0.98	0.99	0.99

TABLE 4 Dispersion values for collapse fragilities of different structural typologies accounting for record-to-record variability alone, modelling uncertainty alone, and a comparison of the SRSS combination of both of these with the total dispersion due to record-to-record variability and modelling uncertainty

Structural Typology	RTR		MDL		TOT		SRSS		TOT/SRSS	
	2 Storey	3 Storey	2 Storey	3 Storey	2 Storey	3 Storey	2 Storey	3 Storey	2 Storey	3 Storey
W/o infill	0.34	0.30	0.33	0.27	0.44	0.45	0.47	0.40	0.92	1.12
Pilotis	0.37	0.38	0.36	0.38	0.44	0.47	0.52	0.54	0.85	0.87
Infill frame (strong)	0.19	0.19	0.20	0.22	0.22	0.25	0.28	0.29	0.79	0.85
Infill frame (weak)	0.17	0.32	0.19	0.34	0.22	0.37	0.25	0.47	0.88	0.81

This discrepancy in the SRSS combination and the observed total dispersion may be due to an assumption of the SRSS combination, which is that the 2 sources of uncertainty are independent of one another. Sufficient data to identify such correlations were not available here due to the limited sample size of the structural typologies, but if it were, the form of the combination would become:

$$\beta^2 = \beta_R^2 + \beta_U^2 - 2\rho\beta_R\beta_U \tag{5.1}$$

where β denotes the total dispersion, β_R denotes the dispersion due to record-to-record variability, β_U denotes the dispersion due to modelling uncertainty, and ρ denotes the correlation between them. By following Equation 5.1 and considering the ratios of the TOT to SRSS-combined dispersions listed in Table 4, it appears that a slight correlation may exist between these 2 sources of uncertainty for the typologies examined here. As mentioned, sufficient data to identify such correlations were not available, and bearing in mind the need to provide simple ways to account for modelling uncertainty in collapse assessment of GLD RC frames in Italy, a more simplified adjustment is proposed. This consists of inflating the dispersion due to record-to-record variability to account for the effects of modelling uncertainty in order to better match the values obtained for both sources of uncertainty (TOT) during analysis using an SRSS combination given by Equation 5.2 rather than use the MDL values listed in Table 4. This is an approximation proposed here that does not require correlation coefficients listed in Equation 5.1 to be quantified. This is done through a prescribed dispersion due to modelling uncertainty ($\beta_{UC,IM}$) to be combined with the existing dispersion values for record-to-record variability ($\beta_{RC,IM}$):

$$\beta_{TOT,IM} = \sqrt{\beta_{RC,IM}^2 + B_{UC,IM}^2} \tag{5.2}$$

The above notation follows that of Cornell et al[6] in order to maintain consistency and to distinguish different types and sources of dispersion. The proposed dispersion values to account for modelling uncertainty are artificially lower that the MDL values to account for the discrepancy listed in Table 4, and these values are listed in Table 5. These were used to modify the RTR collapse fragility functions in Figure 6, and the results were labelled as ADJ in both Figure 6 and Table 5. While this approach is a simplifying compromise more in line with existing guidelines such as FEMA P695, it can be seen to work reasonably well when compared with the collapse fragility considering both sources of uncertainty (TOT).

Comparing these dispersion values to some existing values in the literature, the values for the frames without masonry infill appear reasonable and of the same order of magnitude, with FEMA P695[31] proposing values of $\beta_{UC,IM}$ between 0.10 and 0.50 depending on how well the model represents the actual structural behaviour and how robust that numerical model is. Dolšek,[8] on the other hand, proposed a $\beta_{UC,IM}$ of 0.52, which at first appears a little higher than those listed in Table 5. However, 2 differences that ought to be considered are that this value applies to frames modelled without infill and also that peak ground acceleration is used as the IM, as opposed to $Sa(T_1)$ used here. This difference may explain the increase in dispersion with respect to the values proposed here. Kosič et al[13] noted the total dispersion ($\beta_{TOT,IM}$) for older RC frames without masonry infill to be in the order of 0.34 to 0.52, which are comparable to the values listed in Table 5. In addition, Gokkaya et al[2] proposed a dispersion to account for modelling uncertainty of 0.33 for bare non-ductile frames with no masonry infill in the US, which is similar to the corresponding case here. Further work in Kosič et al[12] segregated the relative contributions for both sources of uncertainty in the collapse capacity of older RC frames and noted a mean value of 0.33 for $\beta_{UC,IM}$ and 0.37 for $\beta_{RC,IM}$, which agree very well with the results presented here in Table 5 for the structural typologies without masonry infill. Compared with the typologies without masonry infill, the collapse dispersion due to modelling uncertainty for the infilled frames seems relatively low. Some comments

TABLE 5 Proposed dispersion values for collapse fragilities of different structural typologies to account for modelling uncertainty and a comparison of the ADJ combination with the total dispersion due to record-to-record variability and modelling uncertainty

Structural Typology	RTR		TOT		Proposed Dispersion ($\beta_{UC,IM}$)	ADJ		TOT/ADJ	
	2 Storey	3 Storey	2 Storey	3 Storey		2 Storey	3 Storey	2 Storey	3 Storey
W/o infill	0.34	0.30	0.44	0.45	0.30	0.45	0.42	0.97	1.06
Pilotis	0.37	0.38	0.44	0.47	0.30	0.47	0.49	0.93	0.96
Infill frame (strong)	0.19	0.19	0.22	0.25	0.15	0.24	0.24	0.90	1.02
Infill frame (weak)	0.17	0.32	0.22	0.37	0.15	0.23	0.35	0.98	1.06

in Kosič et al[12] could help explain this difference where it was noted that shorter period structures tended to have a lower dispersion due to modelling uncertainty, similar to the results reported here (in Table 3.1) for infilled frames. This was attributed by Kosič et al[12] to the higher number of oscillations and more rapid deterioration of the short period systems to result in an IDA trace with a higher "curvature" (see Figure 3 of Kosič et al[12]) compared with longer period systems. This same analogy of short period structures, along with the cliff effect outlined later in Figure 9, that produces higher curvature IDA traces for the infilled frames to give a lower dispersion in collapse capacity is identified here as the perpetrator of this.

5.2 | Influence of modelling uncertainty on demand parameters

While the previous section looked at the influence of modelling uncertainty on collapse, this section discusses the effects on the demand parameters that are typically used for the seismic assessment of structures, namely PSD and PFA. Similar to the approach adopted for the collapse fragility functions, the effects of modelling uncertainty were incorporated by using an SRSS combination with the record-to-record variability to give the overall dispersion in the demand parameters, described by the following expressions:

$$\beta_{D,\theta} = \sqrt{\beta^2_{DR,\theta} + \beta^2_{DU,\theta}} \tag{5.3}$$

$$\beta_{D,a} = \sqrt{\beta^2_{DR,a} + \beta^2_{DU,a}} \tag{5.4}$$

which again assumes that the 2 sources of uncertainty are uncorrelated. The subscript D denotes demand, whereas θ and a refer to PSD and PFA, respectively. Further investigation described in O'Reilly[16] has shown that the use of an SRSS combination gives a good representation, albeit slightly large, of the overall dispersion in the 2 demand parameters. The conservatism is owed to slight correlations that exist between the 2 sources of uncertainty.[6] When the demand and the capacity are correlated, the overall dispersion is reduced, as was the case here. This correlation could also be negative, resulting in an increase in overall dispersion, as noted by Kazantzi and Vamvatsikos.[25] As such, this more simplified and slightly conservative approach of ignoring correlation was deemed appropriate, and trends in the actual dispersion were therefore identified with respect to the various limit states of the buildings, which compute the total dispersion for each demand parameter following Equations 5.3 and 5.4.

In order to compute the dispersion in the 2 demand parameters due to modelling uncertainty, the results were analysed with respect to both ground motion record and model realisation. The dispersion due to modelling uncertainty versus intensity was investigated for both demand parameters at each storey of the case study structures examined. As discussed in Section 2, previous research suggests that the dispersion is not only a function of the demand parameter of interest but also to the limit state being considered, where the limit states described here are as per Figure 3. To account for this, the median intensities associated with each of the 4 limit states estimated using the deterministic model described in Section 4.1 were used here to provide an indication of the relative regions of structural response. Figures 7 and 8 present the dispersion due to modelling parameter type uncertainty versus intensity for both demand parameters, where the median intensity for the 4 limit states considered is shown also.

Some initial comments regarding the values are that the PFA dispersion values tend to be much lower than those of PSD, a trend that is also present in the proposed values of FEMA P58.[7] In addition, the dispersion tends to increase with more severe limit states for the PSD but tends to plateau for the PFA. One reason for this may be due to the structure becoming more non-linear with increasing intensity and thus being influenced by the dispersion in more RVs for the backbone behaviour, whereas the PFAs tend to be capped by the first-mode lateral yield strength of the structure. For instance, consider the dispersion values associated with the PFA in the pilotis frames. The behaviour of these frames was typically governed by the soft-storey forming at the ground storey, and dispersion due to modelling uncertainty for PFA largely came from the dispersion of the lateral capacity of that floor only, meaning that the influential RVs were greatly reduced compared with other frames. This could explain the slightly lower dispersion of the PFA for the pilotis frame with respect to the other frame typologies. In addition, the dispersion in PSD in the upper floors for pilotis frames did not reduce significantly with respect to the ground floor in the same way the drift demands did. Although the median drift demands did decrease in the upper levels, the dispersion of these relatively small values was still comparatively

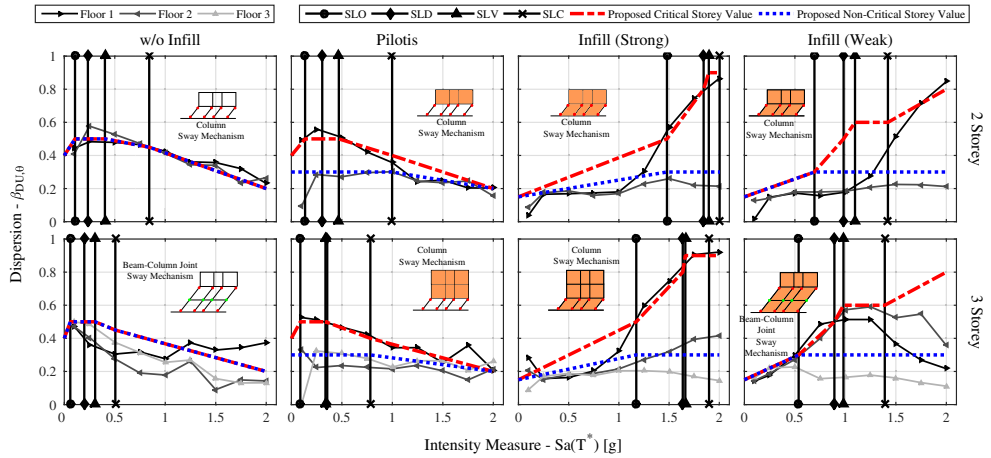

FIGURE 7 Dispersion due to modelling parameter type uncertainty associated with the PSD ($\beta_{DU,\theta}$) versus intensity for the different structural typologies, where the median intensities for the 4 limit states of interest are plotted alongside the proposed values and a distinction has been made between the critical storey and non-critical storey dispersion. In addition, the failure mechanism of each structural typology identified from static pushover analysis using the deterministic model identified in O'Reilly[16] is illustrated in each case [Colour figure can be viewed at wileyonlinelibrary.com]

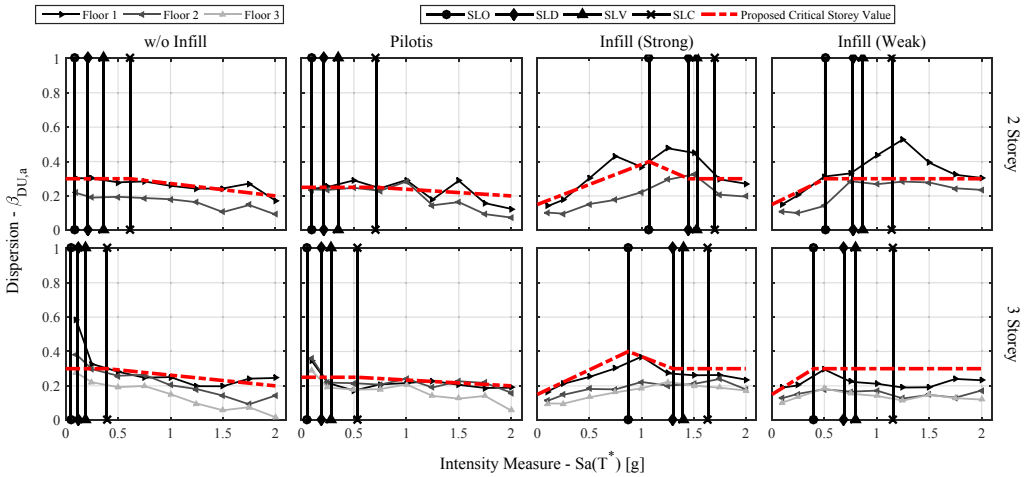

FIGURE 8 Dispersion due to modelling parameter type uncertainty associated with the PFA ($\beta_{DU,a}$) versus intensity for the different structural typologies, where the median intensities for the 4 limit states of interest are plotted alongside the proposed values [Colour figure can be viewed at wileyonlinelibrary.com]

large and would likely not be significant in assessment results. The PSD dispersion tended to reduce for intensities beyond the SLC limit state in the cases of the frames without infill modelling and the pilotis frames. This can be explained conceptually as being due to the structure being highly non-linear, and as a result, the mechanism acted as a fuse where all of the median PSD demand is concentrated. This increase in PSD demand and formation of a mechanism reduced the number of RVs that were directly influencing the overall response of the frame, and as a result, the dispersion reduced with respect to the lower limit states, as illustrated in Figure 7. This reduction is not evident for the infilled frames because the intensities up to which this study was conducted do not surpass the median SLC limit state intensity of the infilled frames very much to identify such a trend, although it is somewhat apparent in the case of the 3-storey weak infill frame.

From the dispersion values identified and shown in Figures 7 and 8 for a given typology and demand parameter, empirical values of dispersion were established approximately by considering the results of both buildings examined and rounding up to the nearest 0.05. Rounding up to 0.05 was chosen as it is in line with guidelines such as FEMA P58. These proposed values are listed in Table 6 in terms of both the structural typology and demand parameter of interest. In addition, a distinction was made in the proposed values between the dispersion associated with the storey

exhibiting a mechanism and the others that do not, which are denoted by the red and blue dashed lines in Figure 7, respectively. This arose due to the frames not being capacity designed and tending to exhibit non-ductile failure modes such as damage to the column members or the beam-column joints. In fact, all of the frames exhibited a soft storey mechanism in the ground floor during static pushover analysis on the deterministic model with median parameter values described in O'Reilly,[16] except for the 3-storey frame without masonry infill and the 3-storey frame with weak infill; both of which exhibited a beam-column joint mechanism at the first floor beam level to result in a shear hinge mechanism that spreads the deformation into the adjacent ground and first storey levels, as previously outlined by Pampanin et al[55] and illustrated in Figure 1. Examining the dispersions in PSD in Figure 7, it was noted that each of the storeys where a mechanism formed corresponds to the locations that exhibit the highest level of dispersion in the PSD demand. To account for this, 2 separate sets of empirical dispersion values were proposed: a critical storey set and a non-critical storey set, and these are both illustrated in Figures 7 and 8 and listed in Table 6. This distinction was made to avoid overestimating the dispersion at the non-critical storeys that tends to be less than that quantified at the critical storey. This represents a specific aspect in seismic assessment of older frames that tend to concentrate the damage at 1 or 2 storeys instead of along the building height like more modern frames. These form a ductile beam-sway mechanism and uniformly distribute the demand more evenly so that a single value of dispersion for each storey demand may be more adequate. For example, in practical applications where only the maximum PSD over the height of the building is utilised (eg, SAC/FEMA methodology[6]), then the dispersion associated with the critical storey should be used. However, in more detailed studies (eg, loss estimation) where the demand parameters at each storey level are required to estimate damage to structural and non-structural elements, a distinction in dispersion between critical and non-critical storeys in older non-ductile frames can be made, as Figure 7 illustrates. Hence, the lower value of dispersion can be adopted for non-critical storeys to avoid overestimating the dispersion in drift demand and subsequently the damage at those levels. As no such trend was observed for the case of the PFA dispersion, no distinction between the different storeys was made. It should also be noted that these values have been developed using low-rise RC frames, and therefore, trends with respect to the number of floors etc have not yet been identified. Future work may be carried out to identify sets of coefficients that are a function of this, or indeed the first-mode period of a structure as was done in FEMA P58,[7] but a single set has been proposed for now. The dispersion values shown in Table 6 should be useful for intensity-based assessments (similar to those done in PACT for FEMA P58,[7] for example). For assessment approaches that instead focus on quantifying the likelihood of exceeding key limit states (such as the displacement based assessment of Welch et al[56]), the relevant dispersion measure would be that of the intensity related to attainment of a specific limit state. This latter type of dispersion should be quantified as part of future research.

TABLE 6 Proposed values (β_{DU}) for both PSD and PFA as a function of structural typology and anticipated median intensity required for the exceedance of each limit state where for PSD, the critical storey value is given alongside the non-critical storey value in parentheses. The different columns represent the different ranges of global structure response where for example, $Sa(T^*)_{SLD} \leq Sa(T^*)$ refers to the intensity levels in which the median SLD limit state intensity ($Sa(T^*)_{SLD}$) has been exceeded

	Modelling Uncertainty (with Reference to Median Intensity NTC 2008 Limit States are Exceeded)					
Structural Typology	$\mathbf{Sa(T^*) < Sa(T^*)_{SLO}}$	$\mathbf{Sa(T^*)_{SLO} \leq Sa(T^*)}$	$\mathbf{Sa(T^*)_{SLD} \leq Sa(T^*)}$	$\mathbf{Sa(T^*)_{SLV} \leq Sa(T^*)}$	$\mathbf{Sa(T^*)_{SLC} \leq Sa(T^*)}$	$\mathbf{Sa(T^*)_{SLC} \leq Sa(T^*)}$
Peak Storey Drift ($\beta_{DU,\theta}$)						
W/o infill	0.40 (0.40)	0.50 (0.50)	0.50 (0.50)	0.50 (0.50)	0.45 (0.45)	0.20 (0.20)
Pilotis frame	0.40 (0.30)	0.50 (0.30)	0.50 (0.30)	0.50 (0.30)	0.40 (0.30)	0.20 (0.20)
Infill frame (strong)	0.15 (0.15)	0.50 (0.30)	0.80 (0.30)	0.90 (0.30)	0.90 (0.30)	0.90 (0.30)
Infill frame (weak)	0.15 (0.15)	0.30 (0.30)	0.50 (0.30)	0.60 (0.30)	0.60 (0.30)	0.80 (0.30)
Peak Floor Acceleration ($\beta_{DU,a}$)						
W/o infill	0.30	0.30	0.30	0.30	0.30	0.20
Pilotis frame	0.25	0.25	0.25	0.25	0.25	0.20
Infill frame (strong)	0.15	0.40	0.30	0.30	0.30	0.30
Infill frame (weak)	0.15	0.30	0.30	0.30	0.30	0.30

Another aspect of the values in Table 6 worth commenting on is the relative magnitude of the PSD dispersion for the infilled frames compared with the frames modelled without infill and pilotis frames. These values were of a much higher magnitude with respect to these other typologies and also with respect to the other non-critical levels in the same structures. Further investigation into both the record-to-record variability and modelling uncertainty in O'Reilly[16] showed that this tended to arise when there was a large peak resistance of the masonry infill to be overcome in order to enter a range of relatively large drift demands, which is illustrated schematically in Figure 9. Upon reaching the peak base shear capacity, the infill strength, and subsequently the overall structural strength, rapidly degraded meaning that the drift demand tended to increase rather significantly depending on the given model realisation or ground motion characteristic. Figure 9 illustrates this for the case of record-to-record variability, where the slight period elongation of an infilled frame due to the onset of structural damage means that depending on the spectral shape and duration of each individual ground motion, the first-mode acceleration demand will differ between ground motion records. This leads to cases where the building period will elongate and shift into a period range with weaker demand than the mean of the ground motion set (Figure 9B), whereas other records may have stronger demand than the mean (Figure 9C). The end result is that there may be instances where the initial period elongation means that sufficient acceleration demand is not inflicted on the building to send the building past its peak and stays in a tight pre-peak band of PSD (Figure 9B), whereas some other ground motions will and result in large values of PSD (Figure 9C). This has been termed the "cliff effect" here, citing an unrelated effect of the same name (also termed, somewhat ironically in this case, the "brick wall

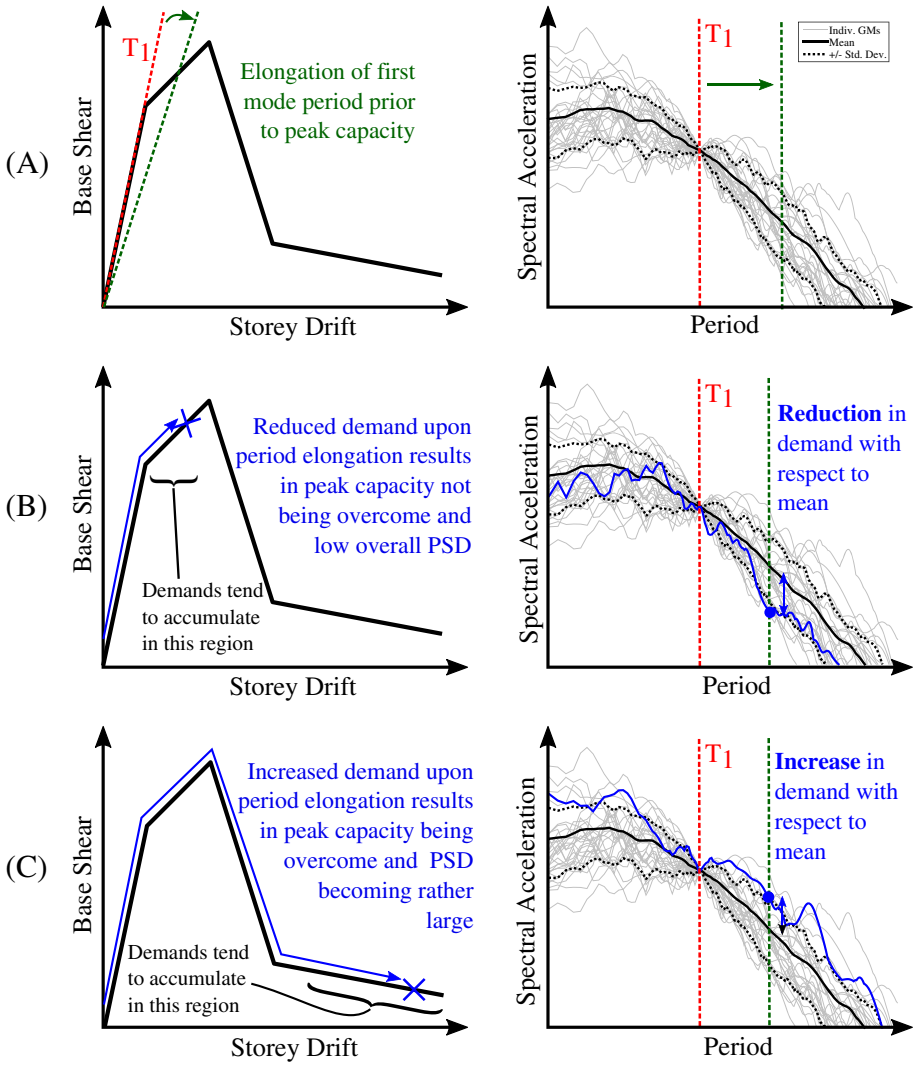

FIGURE 9 Illustration of the impact of the initial peak capacity of the infilled frames on the record-to-record variability in the PSD demands, termed the "cliff effect". Depending on the spectral characteristics of the ground motions conditioned at $Sa(T_1)$, the slight period lengthening close to the peak base shear capacity means that the spectral demands are somewhat different between ground motion records or model realisations and have a significant impact on the PSD demand observed [Colour figure can be viewed at wileyonlinelibrary.com]

effect") that is observed in telecommunications.[57] The analogy is that depending on the ground motion record or model realisation, some records remain in the pre-peak capacity zone of the infilled frame response while others "fall off" from this peak and exhibit relatively large PSD demands in the post peak zone of response.

The so-called "cliff effect" was also identified to be the cause of large dispersion in both the record-to-record variability discussed in O'Reilly[16] and modelling uncertainty for the case of RC frames with masonry infill, being more pronounced for frames with stronger infill typology. It was deemed to apply to any structural system with a similar hysteretic backbone behaviour whereby a significant loss of strength capacity doesn't result in global collapse and allows the structure to keep going past this reduction in strength capacity—such as the case of infilled RC frames. To give an idea of hysteretic backbone proportions, the storey shear contribution ratio from the masonry infill at the critical storey in the strong infill typologies tended to be greater than approximately 0.50 whereas the same ratio was less than 0.50 for the corresponding weak infill typologies. Examining the PSD dispersion due to modelling uncertainty at lower intensities showed that for a relatively low demand, the dispersion remains within an expected range when compared with other frames typologies, but the progression of response into the higher limit states results in a sharp increase in dispersion for the PSD. Again, while the illustration in Figure 9 presents this effect in terms of dispersion due to record-to-record variability—due to it being more intuitive to illustrate for a given model realisation for many ground motions—the same analogy has been identified for dispersion due to modelling uncertainty due to the differences in model realisation for a given ground motion record. The first-mode period and overall capacity among different model realisations lead to numerous model realisations with differing modal and hysteretic backbone properties to attract differing PSD demands depending on the ground motion characteristics to result in a significant difference is maximum PSD demand depending on whether this cliff effect has been observed between model realisations. Furthermore, it was noted that the lognormality of these demand distributions was maintained when performing a Lilliefors test at the 5% significance level. This suggests that the current approach of using $Sa(T_1)$ as an IM is, in fact, quite inefficient for these typologies as it is tied to the T_1 of the structure that has little relevance on the actual structural response once the masonry infill has collapsed and the RC frame yielded. Future research could investigate different IMs that are more efficient by reducing the associated dispersion in the resulting demand parameters. Some potential candidates would be those that are not linked solely to the T_1 of the building, such as those recently proposed[58,59] that define the IM as a function of the spectral demands in range of periods above and below the T_1.

6 | SUMMARY AND CONCLUSIONS

This paper examined the impact of modelling uncertainty on the fragility of GLD RC frames with masonry infill in Italy. Existing research on the general topic of quantifying modelling uncertainty was first reviewed to provide insight into various aspects to be considered. This was then followed by a description of the methodology used to generate the model realisations using the various RVs established for the structural members such that their effects on the collapse fragility and the PSD and PFA demand could be quantified. From this quantification study, the following conclusions can be drawn:

- The effects of modelling uncertainty on the collapse capacity of the GLD RC frame with masonry infill structures showed that the median collapse intensity tends to reduce and the dispersion tends to increase—a finding that is in line with previous research. From the analysis conducted, empirical values for the reduction of the median collapse intensity and the increase in the dispersion for the collapse fragility were provided with respect to each of the structural typologies examined.
- The dispersion of the PSD and PFA of different structural typologies was seen to be increased significantly by model parameter uncertainty. From the analysis of the model realisations generated for each structural typology, a set of empirical dispersion values to account for modelling uncertainty were proposed with respect to the different limit states, structural typology, and the demand parameter of interest. In addition, a distinction was made between the dispersion associated with PSD in critical and non-critical storeys of the frames as the behaviour of the frames was shown to localise the dispersion depending on the location of the mechanism.
- Increased dispersion in PSD demands was observed for GLD RC frames with masonry infills and was attributed to the effects of period elongation pushing some model realisations past the peak lateral resistance point with others remaining in the tightly bound pre-peak region of response. This was termed the "cliff effect," and the large dispersions in PSD for frames with infill were attributed to the large spacing in PSD demands associated with this.

- The increased dispersion associated with modelling uncertainty in GLD RC frames with masonry infills is quantitatively different from other structures such as modern ductile RC frames without masonry infills to the point where default values provided in guidelines such as FEMA P58 cannot be reasonably adopted as these have not considered the different issues associated with the response of GLD frames with masonry infill discussed here.

While the study conducted here has provided a set of default values to quantify the modelling uncertainty in various RC frame typologies, some limitations of this work and possible future directions are noted. Firstly, the number of storeys is a parameter that ought to be investigated further, because the above study considered the modelling uncertainty in just 2 and 3-storey frames. As such, the modelling uncertainty values proposed in Table 6 are to be applied to low-rise buildings and preliminary application to buildings with a larger number of storeys, pending future work. Another issue that has not been considered is the effect of double strut modelling of the masonry infill on the modelling uncertainty. This was not included here due to numerical convergence issues, and trying to achieve a robust model for each realisation proved rather problematic. This is of particular interest as considering the shear behaviour in the columns could be expected to increase the overall dispersion in the demand parameters, although this remains to be investigated further. This consideration would allow for the further investigation of the modelling uncertainty on the expected failure mechanism in the structures, where one would expect that depending on the expected failure mechanism the empirical value of modelling uncertainty may be refined as a function of this. Lastly, model type uncertainty[24,25] has not been considered here and could be a very interesting topic for future work so as to consider the impact of different modelling techniques in addition to model parameters on overall modelling uncertainty.

ACKNOWLEDGEMENTS

The constructive comments of two anonymous reviewers helped improve the overall quality of this paper. The authors would like to acknowledge the funding provided by the IUSS Pavia doctoral programme and the ReLUIS consortium. In addition, the first author wishes to acknowledge the numerous discussions with both David P. Welch and Athanasios Papadopoulos that helped improve the overall quality of the work.

ORCID


Gerard J. O'Reilly http://orcid.org/0000-0001-5497-030X

REFERENCES

1. Cornell CA, Krawinkler H. Progress and challenges in seismic performance assessment. *PEER Center News*. 2000;3(2):1-2.
2. Gokkaya BU, Baker JW, Deierlein GG. Quantifying the impacts of modeling uncertainties on the seismic drift demands and collapse risk of buildings with implications on seismic design checks. *Earthq Eng Struct Dyn*. 2016;45(10):1661-1683. https://doi.org/10.1002/eqe.2740
3. Priestley MJN, Calvi GM, Kowalsky MJ. *Displacement Based Seismic Design of Structures*. Pavia, Italy: IUSS Press; 2007.
4. Fajfar P, Dolšek M. A practice-oriented estimation of the failure probability of building structures. *Earthq Eng Struct Dyn*. 2012;41(3):531-547. https://doi.org/10.1002/eqe.1143
5. Kosič M, Dolšek M, Fajfar P. Pushover-based risk assessment method: a practical tool for risk assessment of building structures. *16th World Conference on Earthquake Engineering*, Santiago, Chile: 2017.
6. Cornell CA, Jalayer F, Hamburger RO, Foutch DA. Probabilistic basis for 2000 SAC federal emergency management agency steel moment frame guidelines. *J Struct Eng*. 2002;128(4):526-533. https://doi.org/10.1061/(ASCE)0733-9445(2002)128:4(526)
7. FEMA P58-1. Seismic Performance Assessment of Buildings: Volume 1—Methodology (P-58-1). vol. 1. Washington, DC: 2012.
8. Dolšek M. Incremental dynamic analysis with consideration of modeling uncertainties. *Earthq Eng Struct Dyn*. 2009;38(6):805-825. https://doi.org/10.1002/eqe.869
9. Celik OC, Ellingwood BR. Seismic fragilities for non-ductile reinforced concrete frames—role of aleatoric and epistemic uncertainties. *Struct Saf*. 2010;32(1):1-12. https://doi.org/10.1016/j.strusafe.2009.04.003
10. Yu X, Lu D, Li B. Estimating uncertainty in limit state capacities for reinforced concrete frame structures through pushover analysis. *Earthq Struct*. 2016;10(1):141-161. https://doi.org/10.12989/eas.2016.10.1.141
11. Celarec D, Ricci P, Dolšek M. The sensitivity of seismic response parameters to the uncertain modelling variables of masonry-infilled reinforced concrete frames. *Eng Struct*. 2012;35:165-177. https://doi.org/10.1016/j.engstruct.2011.11.007

12. Kosič M, Dolšek M, Fajfar P. Dispersions for the pushover-based risk assessment of reinforced concrete frames and cantilever walls. *Earthq Eng Struct Dyn*. 2016;45(13):2163-2183. https://doi.org/10.1002/eqe.2753
13. Kosič M, Fajfar P, Dolšek M. Approximate seismic risk assessment of building structures with explicit consideration of uncertainties. *Earthq Eng Struct Dyn*. 2014;43(10):1483-1502. https://doi.org/10.1002/eqe.2407
14. Kohrangi M, Vamvatsikos D, Bazzurro P. Implications of intensity measure selection for seismic loss assessment of 3-D buildings. *Earthq Spectra*. 2016;32(4):2167-2189. https://doi.org/10.1193/112215EQS177M
15. O'Reilly GJ, Sullivan TJ. Modelling techniques for the seismic assessment of existing Italian RC frame structures. *J Earthq Eng*. 2017;1-35. https://doi.org/10.1080/13632469.2017.1360224
16. O'Reilly GJ. Performance-based seismic assessment and retrofit of existing RC frame buildings in Italy. PhD Thesis, IUSS Pavia, Italy, 2016.
17. O'Reilly GJ, Sullivan TJ. Influence of modelling parameters on the fragility assessment of pre-1970 Italian RC structures. *COMPDYN 2015—5th ECCOMAS Thematic Conference on Computational Methods in Structural Dynamics and Earthquake Engineering*, Crete Island, Greece: 2015. DOI: https://doi.org/10.13140/RG.2.1.4822.8968.
18. O'Reilly GJ, Sullivan TJ. Modelling uncertainty in existing Italian RC frames. *COMPDYN 2017—6th International Conference on Computational Methods in Structural Dynamics and Earthquake Engineering*, Rhodes Island, Greece: 2017.
19. Liel AB, Haselton CB, Deierlein GG, Baker JW. Incorporating modeling uncertainties in the assessment of seismic collapse risk of buildings. *Struct Saf*. 2009;31(2):197-211. https://doi.org/10.1016/j.strusafe.2008.06.002
20. Ellingwood BR, Celik OC, Kinali K. Fragility assessment of building structural systems in mid-America. *Earthq Eng Struct Dyn*. 2007;36(13):1935-1952. https://doi.org/10.1002/eqe.693
21. Kwon OS, Elnashai A. The effect of material and ground motion uncertainty on the seismic vulnerability curves of RC structure. *Eng Struct*. 2006;28(2):289-303. https://doi.org/10.1016/j.engstruct.2005.07.010
22. Dolšek M. Simplified method for seismic risk assessment of buildings with consideration of aleatory and epistemic uncertainty. *Structure and Infrastructure Engineering: Maintenance, Management, Life-Cycle Design and Performance*. 2012;8(10):939-953. https://doi.org/10.1080/15732479.2011.574813
23. EN 1998-1:2004. Eurocode 8: Design of Structures for Earthquake Resistance—Part 1: General Rules, Seismic Actions and Rules for Buildings. Brussels, Belgium: 2004.
24. Bradley BA. A critical examination of seismic response uncertainty analysis in earthquake engineering. *Earthq Eng Struct Dyn*. 2013;42(11):1717-1729. https://doi.org/10.1002/eqe.2331
25. Kazantzi AK, Vamvatsikos D, Lignos DG. Seismic performance of a steel moment-resisting frame subject to strength and ductility uncertainty. *Eng Struct*. 2014;78:69-77. https://doi.org/10.1016/j.engstruct.2014.06.044
26. Terzic V, Schoettler MJ, Restrepo JI, Mahin SA. Concrete column blind prediction contest 2010: outcomes and observations. *PEER Report 2015/01* 2015.
27. Haselton CB, Deierlein GG. Assessing seismic collapse of modern reinforced concrete moment frame buildings. *Blume Report No 156* 2007.
28. Ibarra LF, Medina RA, Krawinkler H. Hysteretic models that incorporate strength and stiffness deterioration. *Earthq Eng Struct Dyn*. 2005;34(12):1489-1511. https://doi.org/10.1002/eqe.495
29. Vamvatsikos D, Fragiadakis M. Incremental dynamic analysis for estimating seismic performance sensitivity and uncertainty. *Earthq Eng Struct Dyn*. 2010;39(2):141-163. https://doi.org/10.1002/eqe.935
30. Jalayer F, Iervolino I, Manfredi G. Structural modeling uncertainties and their influence on seismic assessment of existing RC structures. *Struct Saf*. 2010;32(3):220-228. https://doi.org/10.1016/j.strusafe.2010.02.004
31. FEMA P695. Quantification of Building Seismic Performance Factors. Washington, DC, USA: 2009.
32. Vamvatsikos D, Cornell CA. Direct estimation of seismic demand and capacity of multidegree-of-freedom systems through incremental dynamic analysis of single degree of freedom approximation. *J Struct Eng*. 2005;131(4):589-599. https://doi.org/10.1061/(ASCE)0733-9445(2005)131:4(589)
33. Galli M. Evaluation of the seismic response of existing RC frame buildings with masonry infills. MSc Thesis, IUSS Pavia, Italy, 2006.
34. Regio Decreto. Norme per l'esecuzione delle opere conglomerato cementizio semplice od armato—2229/39. Rome, Italy: 1939.
35. Vona M, Masi A. Resistenza sismica di telai in c.a. progettati con il R.D. 2229/39. XI Congresso Nazionale "L'Ingegneria Sismica in Italia," vol. 3274, Genova, Italia: 2004.
36. Sassun K, Sullivan TJ, Morandi P, Cardone D. Characterising the in-plane seismic performance of infill masonry. *Bulletin of the New Zealand Society for Earthquake Engineering* 2015; 49(1).
37. Haselton CB, Goulet CA, Mitrani Reiser J, Beck JL, Deierlein GG, Porter KA, *et al*. An assessment to benchmark the seismic performance of a code-conforming reinforced concrete moment-frame building. *PEER Report 2007/12* 2007.
38. McKenna F, Fenves G, Filippou FC, Mazzoni S. Open system for earthquake engineering simulation (OpenSees) 2000. http://opensees.berkeley.edu/wiki/index.php/Main_Page.

39. Crisafulli FJ, Carr AJ, Park R. Analytical modelling of infilled frame structures—a general review. *Bulletin of the New Zealand Society for Earthquake Engineering* 2000; 33(1): 30–47.
40. Bacco V. Solaio in latero-cemento: Confronto con sistemi alternativi 2009. http://www.solaioinlaterizio.it/user/ConfrontoAlternativi.pdf.
41. Hak S, Morandi P, Magenes G, Sullivan TJ. Damage control for clay masonry infills in the design of RC frame structures. *J Earthq Eng*. 2012;16(sup1):1-35. https://doi.org/10.1080/13632469.2012.670575
42. Vamvatsikos D, Cornell CA. Incremental dynamic analysis. *Earthq Eng Struct Dyn*. 2002;31(3):491-514. https://doi.org/10.1002/eqe.141
43. Vamvatsikos D, Cornell CA. Applied incremental dynamic analysis. *Earthq Spectra*. 2004;20(2):523-553. https://doi.org/10.1193/1.1737737
44. Sullivan TJ, Welch DP, Calvi GM. Simplified seismic performance assessment and implications for seismic design. *Earthq Eng Eng Vib*. 2014;13(Supp1):95-122. https://doi.org/10.1007/s11803-014-0242-0
45. O'Reilly GJ, Sullivan TJ. Probabilistic seismic assessment and retrofit considerations for Italian RC frame buildings. *Bulletin of Earthquake Engineering* 2017(Under Review).
46. NTC. *Norme Tecniche Per Le Costruzioni*. Rome, Italy: 2008.
47. Seismic VD. Performance uncertainty estimation via IDA with progressive accelerogram-wise Latin hypercube sampling. *J Struct Eng*. 2014;140(8):A4014015. https://doi.org/10.1061/(ASCE)ST.1943-541X.0001030
48. Ugurhan B, Baker JW, Deierlein GG. Uncertainty estimation in seismic collapse assessment of modern rein- forced concrete moment frame building. *10th National Conference in Earthquake Engineering*, Anchorage, AK: 2014.
49. Haselton CB, Liel AB, Taylor Lange S, Deierlein GG. Beam-column element model calibrated for predicting flexural response leading to global collapse of RC frame buildings. *PEER Report 2007/03* 2008.
50. McKay MD, Beckman RJ, Conover WJ. A comparison of three methods for selecting values of input variables in the analysis of output from a computer code. *Dent Tech*. 1979;21(2):239-245.
51. Olsson A, Sandberg G, Dahlblom O. On Latin hypercube sampling for structural reliability analysis. *Struct Saf*. 2003;25(1):47-68. https://doi.org/10.1016/S0167-4730(02)00039-5
52. Mathworks. Version 8.3.0 (R2014a). Natick, Massachusetts: The Mathworks Inc.; 2014.
53. Owen AB. Controlling correlations in Latin hypercube samples. *J Am Stat Assoc*. 1994;89(428):1517. https://doi.org/10.2307/2291014
54. Baker JW. Efficient analytical fragility function fitting using dynamic structural analysis. *Earthq Spectra*. 2015;31(1):579-599. https://doi.org/10.1193/021113EQS025M
55. Pampanin S, Magenes G, Carr AJ. "Modelling of Shear Hinge Mechanism in Poorly Detailed RC Beam/Column Joints", fib Symposium on Concrete Structures in Seismic Regions, Athens, paper n.171, 2002.
56. Welch DP, Sullivan TJ, Calvi GM. Developing direct displacement-based procedures for simplified loss assessment in performance-based earthquake engineering. *J Earthq Eng*. 2014;18(2):290-322. https://doi.org/10.1080/13632469.2013.851046
57. Doel G. DVB-T transmission systems. ITU/ASBU Workshop on Frequency Planning and Digital Transmission, Damascus, Syria: 2004.
58. Kohrangi M, Vamvatsikos D, Bazzurro P. Site dependence and record selection schemes for building fragility and regional loss assessment. *Earthq Eng Struct Dyn*. 2017;46(10):1625-1643. https://doi.org/10.1002/eqe.2873
59. Eads L, Miranda E, Lignos DG. Average spectral acceleration as an intensity measure for collapse risk assessment. *Earthq Eng Struct Dyn*. 2015;44(12):2057-2073. https://doi.org/10.1002/eqe.2575

How to cite this article: O'Reilly GJ, Sullivan TJ. Quantification of modelling uncertainty in existing Italian RC frames. *Earthquake Engng Struct Dyn*. 2018;47:1054–1074. https://doi.org/10.1002/eqe.3005